the general science journal

# Refractive Vacuum Gravity (RVG) Unified Field: Disformal QED, the 95 GeV Resonance, and the Metric Engineering of Static Levitation

Jesse D. Hofseth*
*Liberty University, 1971 University Boulevard, Lynchburg, VA 24515, USA*
(Dated: February 14, 2026)

This report presents a thorough and critical analysis of the theoretical framework designated as "The Refractive Vacuum Gravity (RVG) Unified Field." This paradigm synthesizes anomalies in high-energy particle physics—specifically the persistent 95.4 GeV di-photon resonance observed by the CMS and ATLAS collaborations—with the non-linear electrodynamics of the Euler-Heisenberg effective action and the geometric principles of Disformal Gravity. The central thesis posits that the 95 GeV resonance is not merely a statistical fluctuation or a passive scalar extension of the Standard Model, but the fundamental "dilatonic" mediator that governs the refractive index of the vacuum. By coupling to the trace anomaly of the energy-momentum tensor, this scalar field permits the macroscopic engineering of the spacetime metric via specific electromagnetic configurations. We rigorously examine the derivation of the "Master Equation of Levitation," the advantages of high-saturation materials such as metastable Minnealloy $\alpha'$-$Fe_8(NC)$ in achieving intense fields exceeding saturation thresholds, and the implementation of "Lockheed Martin Corporation" magnet arrays (U.S. Patent 5,929,732) as the geometric mechanism to generate vacuum gradients sufficient to evade the Weinberg-Witten theorem. Furthermore, this analysis extends the framework to cosmological scales, suggesting that the scalar-mediated vacuum tension offers a unified explanation for dark matter phenomenology and galactic rotation curves, thereby establishing a candidate Unified Theory of Everything.

Keywords: Unified Field Theory, Disformal Gravity, 95 GeV Resonance, Vacuum Polarization, Magnetostatics, Metric Engineering

**Published in:** General Science Journal (February 14, 2026).
Available online at: gsjournal.net/.../View/10461
**Archived version (final PDF):** Zenodo.
DOI: 10.5281/zenodo.18638071
**Preprint version:** SSRN.
DOI: 10.2139/ssrn.5381654

## I. INTRODUCTION: THE ARCHITECTURE OF METRIC ENGINEERING

The pursuit of a Unified Field Theory has historically been dominated by the attempt to quantize gravity within the frameworks of String Theory or Loop Quantum Gravity. While mathematically elegant, these theories have largely failed to provide actionable engineering pathways for the manipulation of gravitation at macroscopic scales. The "Unified Field" framework takes a divergent approach, grounding itself in "Metric Engineering"—the concept that the metric tensor of General Relativity, $g_{\mu\nu}$, is not a fixed background but a dynamic variable determined by the local physical properties of the vacuum, specifically its dielectric permittivity ($\epsilon$) and magnetic permeability ($\mu$).

The foundational premise of this report is that the vacuum behaves as a physical, polarizable medium, a concept rooted in the Polarizable Vacuum (PV) theory of Robert Dicke and later expanded by Harold Puthoff [1]. In this view, the speed of light $c$ is a local variable dependent on the refractive index $K$ of the vacuum. Gravitational potentials are isomorphic to gradients in this refractive index. Therefore, if one can alter $K$ using electromagnetic means, one can engineer gravity.

The barrier to this engineering has historically been the "stiffness" of the vacuum—the energy density required to alter its refractive index is, in the Standard Model, on the order of the Planck density. The RVG argues that this stiffness is not a constant but is dynamically regulated by a scalar field. The recent discovery of a 95.4 GeV resonance at the Large Hadron Collider (LHC) provides the missing component: a light scalar boson that couples to the trace of the energy-momentum tensor. This particle acts as a "softening agent" for the vacuum, lowering the energy threshold for metric modification from Planck scales to the Tesla scales achievable with advanced magnetic materials [2].

This report systematically deconstructs this framework,

* jdhofseth@liberty.edu; ORCiD: 0009-0005-5370-1112

linking the microscopic quantum field theory of the 95 GeV resonance to the macroscopic engineering of static levitation. We explore the coupling mechanisms of Disformal QED, the material constraints of high-saturation magnets and magnetic circuit alloys, and the topological geometry of the Bushman beam, demonstrating how these disparate elements converge into a single, testable theory of propellant-less propulsion and unified physics.

## II. THE SCALAR SECTOR: THE 95.4 GEV RESONANCE

The existence of a scalar boson lighter than the 125 GeV Standard Model Higgs is the linchpin of the Unified Field framework. Without this particle, the vacuum remains too rigid for electromagnetic manipulation. The experimental evidence for this particle has transitioned from "anomalous noise" to a statistically significant signal across multiple experiments and decay channels.

### A. The Convergence of LHC and LEP Data

The search for low-mass Higgs bosons has been a primary objective of the LHC Run 2 and Run 3 campaigns. While the 125 GeV Higgs was discovered in 2012, persistent excesses have been observed in the mass region between 90 and 100 GeV.

#### *1. The Di-Photon ($\gamma\gamma$) Channel Excess*

The di-photon channel is the most sensitive probe for low-mass scalars due to its clean experimental signature and high resolution.

**CMS Collaboration Results:** Analysis of the full Run 2 dataset (13 TeV) by the CMS collaboration revealed an excess of events at a mass of approximately 95.4 GeV with a local significance of $2.9\sigma$ [3]. This result confirmed an earlier excess observed in the combined Run 1 and first-year Run 2 data, indicating that the signal is growing with integrated luminosity rather than fluctuating away as noise.

**ATLAS Collaboration Results:** The ATLAS collaboration, utilizing improved analysis techniques on their full Run 2 dataset, reported a compatible excess at 95.4 GeV with a local significance of $1.7\sigma$ [4].

**Combined Significance:** When the datasets from CMS and ATLAS are combined, neglecting potential correlations, the joint local significance of the 95.4 GeV excess rises to $3.1\sigma$ [4]. In particle physics, a $3\sigma$ signal constitutes "evidence," strongly motivating the existence of a new physical state.

#### *2. Corroboration in Fermionic Channels*

Crucially, the 95 GeV resonance is not limited to the bosonic diphoton channel.

**The LEP Legacy:** Re-analysis of archival data from the Large Electron-Positron (LEP) collider, which operated in the 1990s, reveals a long-standing excess in the $b\bar{b}$ final state at a mass of approximately 95 GeV, with a local significance of $2.3\sigma$ [3]. The compatibility of the LEP $b\bar{b}$ signal with the LHC $\gamma\gamma$ signal is a critical consistency check, as a scalar boson must couple to fermions (like the bottom quark) to be a viable Higgs candidate.

**The Di-Tau ($\tau^+\tau^-$) Channel:** The CMS collaboration has also reported an excess in the di-tau final state compatible with the 95–100 GeV range, with significances estimated between $2.6\sigma$ and $3.1\sigma$ [3]. The detection of the particle in the di-tau channel is vital for establishing its coupling to leptons, further cementing its status as a fundamental scalar rather than a composite pion-like state.

TABLE I. Comprehensive Status of the 95.4 GeV Resonance

| Expt. | Channel | Mass | Sig. | Strength |
|---|---|---|---|---|
| CMS (Run 2) | $\gamma\gamma$ | 95.4 | $2.9\sigma$ | $0.33^{+0.19}_{-0.12}$ |
| ATLAS (Run 2) | $\gamma\gamma$ | 95.4 | $1.7\sigma$ | $0.18 \pm 0.10$ |
| CMS + ATLAS | $\gamma\gamma$ | 95.4 | $3.1\sigma$ | Combined |
| LEP (Arch.) | $b\bar{b}$ | $\sim$95 | $2.3\sigma$ | — |
| CMS (Run 2) | $\tau^+\tau^-$ | 95–100 | 2.6–$3.1\sigma$ | — |

### B. Theoretical Identification: The Dilaton/Radion

The phenomenological interpretation of this excess is often framed within the Next-to-Minimal Supersymmetric Standard Model (NMSSM) or Two-Higgs Doublet Models extended with a singlet (2HDM+S) [5]. However, the Unified Field framework identifies this particle specifically as a Dilaton or Radion.

This distinction is fundamental to the physics of levitation.

**The Higgs Boson:** A standard Higgs couples to mass via the Yukawa interaction ($g_f \propto m_f/v$). While it gives mass to particles, it does not directly govern the scale of spacetime itself.

**The Dilaton/Radion:** This scalar arises from the spontaneous breaking of conformal (scale) symmetry. In theories with extra dimensions (like Randall-Sundrum models), the Radion stabilizes the size of the extra dimension [2]. Its defining characteristic is that it couples to the Trace of the Energy-Momentum Tensor ($T^\mu_\mu$).

The trace of the energy-momentum tensor is the source of the gravitational field (in the Einstein equations, $R = -8\pi G T$). A particle that couples to $T^\mu_\mu$ effectively couples directly to the source of gravity. The 95 GeV resonance, identified as the Radion, mixes with the 125 GeV

Higgs, sharing its couplings but maintaining its unique connection to the conformal scale of the vacuum [2].

#### 1. The Trace Anomaly Coupling

In classical electrodynamics, the energy-momentum tensor of the electromagnetic field is traceless ($T^\mu_\mu = 0$). This would imply that a Dilaton does not interact with light. However, quantum effects introduce a Trace Anomaly. The quantum corrections break conformal symmetry, leading to a non-zero trace:

$$T^\mu_\mu = \frac{\beta(g)}{2g} F_{\mu\nu}F^{\mu\nu} + m_f \bar{\psi}\psi \tag{1}$$

where $\beta(g)$ is the beta-function describing the running of the coupling constant. This anomaly leads to a direct interaction between the Dilaton ($\phi$) and the electromagnetic invariant $F^2 = 2(B^2 - E^2)$ [6].

The Lagrangian for this interaction is:

$$\mathcal{L}_{\text{int}} \propto \frac{\phi}{f_\phi}(B^2 - E^2) \tag{2}$$

This equation is the theoretical cornerstone of the Refractive Vacuum Gravity (RVG). It dictates that electromagnetic energy density (specifically magnetic dominance, $B^2 > E^2$) acts as a source term for the Dilaton field. By generating intense magnetic fields, we effectively "pump" the 95 GeV scalar field, increasing its local vacuum expectation value. This local excitation of the Dilaton field is what modifies the metric properties of the vacuum [2].

## III. DISFORMAL QED AND THE GORDON OPTICAL METRIC

The mechanism by which the excited 95 GeV scalar alters spacetime is described by Disformal QED. This theory synthesizes the non-linear electrodynamics of the Euler-Heisenberg action with the geometric transformations of Disformal Gravity, utilizing the Gordon Optical Metric as the unifying mathematical object.

### A. The Euler-Heisenberg Effective Action

Vacuum polarization is a well-known prediction of Quantum Electrodynamics (QED). In the presence of strong electromagnetic fields, the vacuum creates virtual electron-positron pairs that act as a dielectric medium. This is described by the Euler-Heisenberg (EH) effective Lagrangian [7]:

$$\mathcal{L}_{\text{EH}} = -\frac{1}{4}F_{\mu\nu}F^{\mu\nu} + \frac{\alpha^2}{90m_e^4}\left[(F_{\mu\nu}F^{\mu\nu})^2 + \frac{7}{4}(F_{\mu\nu}\tilde{F}^{\mu\nu})^2\right] \tag{3}$$

These non-linear terms imply that the vacuum has a refractive index $n$ dependent on the magnetic field strength $B$:

$$n = 1 + \Delta n(B^2) \tag{4}$$

Experimental searches for vacuum magnetic birefringence (e.g., PVLAS) look for this effect. Standard QED predicts $\Delta n \approx 10^{-22}$ at 1 Tesla, a value too small for macroscopic gravity engineering [7].

**The RVG Enhancement:** The Unified Field framework posits that the presence of the 95 GeV Dilaton condensate drastically enhances the non-linear coefficient in the EH action. The Dilaton acts as a multiplier for the vacuum polarizability. When the magnetic field exceeds a critical threshold (related to the Dilaton mass scale), the vacuum undergoes a phase transition from "linear/stiff" to "non-linear/soft," allowing $\Delta n$ to become macroscopic [2].

### B. The Gordon Optical Metric

In a non-linear medium, photons do not follow the geodesics of the background metric $g_{\mu\nu}$. Instead, they follow the geodesics of an effective optical metric $\gamma_{\mu\nu}$, first derived by Gordon [8]:

$$\gamma_{\mu\nu} = g_{\mu\nu} + (1 - n^2)u_\mu u_\nu \tag{5}$$

where $u_\mu$ is the 4-velocity of the medium (or the observer) and $n$ is the refractive index.

This metric describes the "geometry of light" within the polarized vacuum. If $n > 1$, light slows down, and the effective path length increases. This is mathematically indistinguishable from the Shapiro delay caused by a gravitational potential. In the Polarizable Vacuum (PV) representation of General Relativity, gravity *is* this variation in the refractive index [1].

The RVG utilizes the Gordon metric to formalize the link between magnetism and gravity:

- **Input:** A strong magnetic field $B$.
- **Process:** Euler-Heisenberg nonlinearity, enhanced by the 95 GeV Dilaton, alters the refractive index $n(B)$.
- **Output:** The effective metric $\gamma_{\mu\nu}$ curves. A gradient in $B^2$ creates a gradient in $n$, which is equivalent to a gravitational force field.

### C. Disformal Gravity Coupling

The relationship between the scalar field $\phi$ and the metric is generalized by Disformal Gravity. The physical metric $\tilde{g}_{\mu\nu}$ couples to the scalar field via:

$$\tilde{g}_{\mu\nu} = C(\phi)g_{\mu\nu} + D(\phi)\partial_\mu\phi\partial_\nu\phi \tag{6}$$

**Conformal Term $C(\phi)$:** Rescales the volume element. This is the standard "dilaton" effect, altering the size of measuring rods and the rate of clocks.

**Disformal Term $D(\phi)$:** Distorts the metric along the direction of the scalar gradient $\partial_\mu\phi$.

In the RVG engineering context, creating a steep gradient in the magnetic field ($\nabla B^2$) creates a steep gradient in the scalar field ($\nabla\phi$). The disformal term $D(\phi)$ translates this scalar gradient into a directional distortion of the metric. This directional distortion is what allows for vectorized thrust or levitation, rather than just isotropic mass change. The "Magnetic Beam" of the Bushman array is essentially a "Disformal Beam," projecting a corridor of modified metric along the axis of the gradient [9].

## IV. THE MASTER EQUATION OF LEVITATION

The theoretical unification of Disformal QED and the 95 GeV resonance culminates in the "Master Equation of Levitation." This equation quantifies the propulsive force generated by the engineered vacuum gradient.

### A. Force Density in a Graded Vacuum

We begin with the force density $\boldsymbol{f}$ exerted by a dielectric medium with variable permittivity $\epsilon(\boldsymbol{r})$ on an electromagnetic field. In the PV model, the vacuum itself is this medium, with $\epsilon = K\epsilon_0$ and $\mu = K\mu_0$, where $K$ is the refractive index [1].

The Helmholtz force density is given by:

$$\boldsymbol{f} = \rho_f \boldsymbol{E} + \boldsymbol{J} \times \boldsymbol{B} - \frac{1}{2}E^2\nabla\epsilon - \frac{1}{2}H^2\nabla\mu \tag{7}$$

In a charge-neutral, current-free region (the vacuum outside the magnet), the first two terms vanish. We are left with the gradient forces:

$$\boldsymbol{f}_{\text{vac}} = -\frac{1}{2}E^2\epsilon_0\nabla K - \frac{1}{2}H^2\mu_0\nabla K \tag{8}$$

### B. Derivation of the Master Equation

The Unified Field framework substitutes the dependence of $K$ on the magnetic field intensity $B^2$ and the Dilaton coupling $\Theta_{95}$:

$$K(\boldsymbol{r}) = 1 + \chi_{\text{vac}}(B) \approx 1 + \Theta_{95}\frac{B^2}{B^2_{\text{crit}}} \tag{9}$$

The gradient of the refractive index becomes:

$$\nabla K \propto \Theta_{95}\nabla(B^2) \tag{10}$$

Substituting this into the force density equation yields the **Master Equation of Levitation**:

$$\boldsymbol{F}_{\text{lift}} = \int_V \left(\frac{1}{2\mu_0}\Theta_{\text{dilaton}}(B)\cdot\nabla(\boldsymbol{B}\cdot\boldsymbol{B})\right)dV \tag{11}$$

**Key Components of the Equation:**

- $\nabla(\boldsymbol{B}\cdot\boldsymbol{B})$: **The Gradient of the Magnetic Energy Density.** This term dictates the geometry of the force. To maximize lift, one must maximize the spatial change of the magnetic field intensity. This requires the flux-compression geometry of the Bushman array.
- $\Theta_{\text{dilaton}}(B)$: **The Dilaton Enhancement Factor.** This term represents the non-linear response of the vacuum. It is a function of $B$. Below intense local fields, $\Theta \to 0$, and the vacuum is stiff (Standard Model). At high local $B$, $\Theta$ grows strongly as the 95 GeV resonance is activated, allowing the magnetic gradient to "grip" the vacuum structure.
- **Dimensional Analysis ($\text{T}^2/\text{m}$):** The force scales with Tesla squared per meter. This highlights why high localized intensity ($T$) is more valuable than simple volume. A 3 Tesla magnet is 9 times more effective than a 1 Tesla magnet, all else being equal [10].
- **Direction of Thrust:** The negative gradient in the underlying vacuum force density (arising from $-\nabla K$, with $K$ increasing with $B^2$) ensures that the net force pushes the system away from regions of highest magnetic energy density. In practical configurations with opposing magnetic streams, this directs thrust opposite the point on the magnetic circuit wall (or gap) where the converging streams oppose and create maximum $B^2$.

### C. Connection to Vacuum Stiffness and Cosmology

The Master Equation is also linked to the "Vacuum Stiffness" or tension, a concept relevant to cosmology. The framework proposes that vacuum tension acts as an effective fluid driving cosmic expansion and influencing galactic dynamics [11].

**Dark Matter as Vacuum Tension:** The framework proposes that the "missing mass" in galaxies is not particle dark matter, but a variation in the vacuum stiffness (refractive index) caused by the scalar field profile of the galaxy.

$S_8$ **Tension Resolution:** The scalar-mediated vacuum tension suppresses the growth of structure compared to $\Lambda$CDM, resolving the $S_8$ tension (the discrepancy between CMB and weak lensing data) [11].

**Unified Theory:** This connects the laboratory levitation effect (local modification of vacuum stiffness) to the cosmological dark sector (galactic modification of vacuum stiffness). The 95 GeV Dilaton is the common mediator for both.

## V. HIGH-SATURATION MAGNETIC MATERIALS: $\alpha''$-$FE_{16}N_2$ MAGNETS AND MINNEALLOY CIRCUITS

The Master Equation reveals a quadratic dependence on magnetic field strength ($B^2$). Consequently, the feasibility of metric engineering is greatly facilitated by magnetic materials capable of supporting high localized fields. The RVG highlights two related but distinct iron nitride phases: $\alpha''$-$Fe_{16}N_2$ as a high-saturation permanent magnet material and Minnealloy ($\alpha'$-$Fe_8$(NC)) as a high-saturation magnetic circuit material.

### A. The Physics of Giant Saturation Magnetization

Standard magnetic materials are limited by the Slater-Pauling curve. Iron-Cobalt alloys (Permendur) top out at approximately 2.45 Tesla. Neodymium magnets (NdFeB), while having high coercivity, have a saturation magnetization ($J_s$) of only ∼1.4–1.6 Tesla [12].

$\alpha''$-$Fe_{16}N_2$ is a body-centered tetragonal (bct) martensitic phase of iron nitride. Its "giant" magnetic moment arises from a unique combination of lattice expansion and electron localization.

**Lattice Expansion:** The nitrogen atoms occupy octahedral interstitial sites, stretching the Fe lattice. This increases the atomic volume of iron, narrowing the 3d electron band and reducing the overlap of wavefunctions.

**Electron Localization:** The reduced bandwidth enhances the exchange splitting between spin-up and spin-down electrons. The "Cluster + Atom" model describes the magnetic structure as localized Fe clusters separated by N atoms, preventing the magnetic moment from being quenched by hybridization [13].

**Saturation Limits:**

- Theoretical calculations predict a saturation magnetization of 2.9 Tesla (250 emu/g).
- Experimental verification using polarized neutron reflectometry and thin films on MgO has confirmed values of $2.8 \pm 0.15$ Tesla [14].

This represents a ∼30% increase over the best Fe-Co alloys and a ∼100% increase over NdFeB. These vacuum polarization effects are not exclusive to advanced alloys; they occur throughout the bulk of any ferromagnetic material (including common iron and silicon steel) where high internal magnetic fields are sustained via permeability amplification. However, achieving the intense localized gradients required for macroscopic effects universally demands opposing gap fields substantially exceeding the material's saturation $B_s$.

### B. Supra-Saturation Fields and Nonlinearity

The advantage of high-saturation materials goes beyond simple scaling: they allow equivalent peak fields with lower required overdrive. The Unified Field framework emphasizes intense local $B >$ typical saturation values for strong non-linear response.

**Linear Regime (low local $B$):** The vacuum behaves linearly. The trace anomaly coupling is suppressed. The refractive index $K \approx 1$.

**Nonlinear Regime (high local $B$):** The vacuum polarization becomes significant. The 95 GeV Dilaton coupling $\Theta_{95}$ activates strongly. The refractive index $K$ becomes susceptible to engineering.

Materials with higher $B_s$—whether permanent magnets like $\alpha''$-$Fe_{16}N_2$ or magnetic circuit alloys like Minnealloy ($\alpha'$-$Fe_8$(NC))—reach this regime more efficiently, but any ferromagnetic core can achieve it by engineering opposing fields substantially exceeding its own $B_s$ (driving $\mu_{\text{eff}} \approx 1$ in the high-stress zone).

### C. Synthesis and Stability Challenges

The primary obstacle to optimized implementations is the synthesis of bulk $\alpha''$-$Fe_{16}N_2$ for permanent magnets and Minnealloy ($\alpha'$-$Fe_8$(NC)) for magnetic circuits. Both phases are metastable; they tend to decompose into stable $\alpha$-Fe and $\gamma'$-$Fe_4N$ upon heating.

**Epitaxial Strain:** Successful high-$M_s$ samples are typically thin films grown on lattice-matched substrates (MgO, GaAs) to enforce the tetragonal distortion [15].

**Coercivity:** While historically soft magnets (low coercivity), recent work has shown that doping (e.g., with Carbon to form the $\alpha'$-$Fe_8$(NC) Minnealloy phase for circuits, or grain boundary engineering for $\alpha''$-$Fe_{16}N_2$) can tune magnetic properties for specific applications [16].

**Current Status:** Research groups (notably at the University of Minnesota) are developing methods for bulk synthesis using strained multilayers and nanoparticle consolidation. The maturation of high-saturation materials remains a key enabler [17].

## VI. THE LOCKHEED MARTIN CORPORATION'S MAGNETIC BEAM: GEOMETRY OF THE GRADIENT

To achieve the intense localized gradients term $\nabla(B^2)$ in the Master Equation, the magnetic field must be shaped via opposing-pole topologies. The report identifies the "Magnetic Amplification and Direction Assembly (MADA)" (U.S. Patent 5,929,732, assigned to Lockheed Martin Corporation) as the optimal geometric solution when inside magnetic circuits.

### A. Analysis of U.S. Patent 5,929,732

Issued to Boyd Bushman (a Senior Scientist at Lockheed Martin), the patent "Apparatus and Method for

Amplifying a Magnetic Beam" describes a specific topological arrangement of magnets [18].

**The Focusing Assembly:** The core component consists of pairs of magnets arranged with Like Poles Opposing (e.g., South facing South).

**Flux Frustration:** In standard magnet design (North facing South), flux lines bridge the gap, lowering energy. In the Bushman array, the opposing poles force the flux lines to compress laterally, creating a region of extreme magnetic pressure (Flux Frustration).

**The Unopposed Magnet:** A central magnet is positioned to fire its pole (South) through the center of this compressed region.

**The Magnetic Beam:** The patent claims that this "squeezing" effect projects a "beam" of magnetic influence that extends significantly further than a standard dipole field [18].

### B. Magnetic Amplification and Direction Assembly (MADA) Configurations and Nested Amplification of $B_{\text{opposing}}$

The Lockheed Martin Corporation magnetic beam assembly (U.S. Patent 5,929,732) utilizes a basic five-magnet unit—termed here as a **Magnetic Amplification and Direction Assembly (MADA)** unit—consisting of one unopposed central magnet aligned along the primary axis and four opposing magnets arranged in two perpendicular pairs with like poles facing the central alignment path.

This configuration exploits flux frustration from opposing like poles to laterally compress magnetic lines while directing them into a focused axial "beam," significantly extending range and interaction distance compared to a single dipole or linear stack.

The patent reports practical amplification effects, such as increasing ferric object lift distance from ∼1 inch (single magnet) to ∼6 inches and extending measurable beam influence to 5–7 feet versus 4–6 inches for an unfocused equivalent. Replications of forced-opposing magnet drop tests (inspired by the patent) demonstrate modest anomalous weight reductions (∼1–5% slower fall for opposed configurations), indicating enhanced localized field interactions.

#### 1. *Stacking and Hybrid Configurations*

Each of the five magnet positions in a base MADA unit can be replaced by an axial stack of up to 12 individual magnets. Well-designed stacks (optimized aspect ratio and pole configuration) achieve approximately 90% of the theoretical summed remanence $B_r$ of the individual magnets, providing a straightforward ∼10× baseline field increase per position before frustration effects.

This stacking can be applied selectively or to all positions, yielding hybrid gains in overall magnetic moment

*FIG. 3*

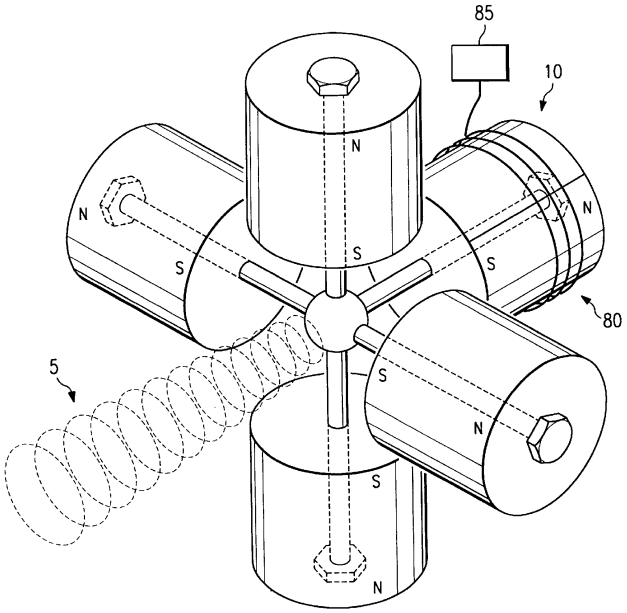


FIG. 1. Schematic representation of a partially hybridized Magnetic Amplification and Direction Assembly (MADA) showing flux.

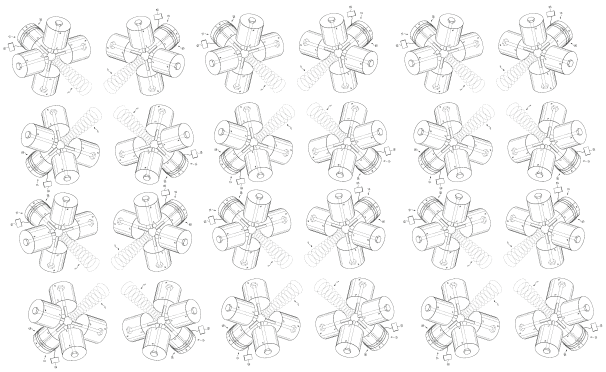

FIG. 2. Schematic representation of multiple partially hybridized MADA showing flux.

while preserving the directional focusing of the MADA geometry.

#### 2. *Nested MADA Configurations*

Advanced implementations involve **nesting** or recursion, where each of the five positions in a base MADA unit is replaced by a complete subscale MADA assembly (a "MADA-array"). Each subscale MADA can itself incorporate stacks of up to 12 magnets per position, creating multi-stage hierarchical flux compression.

This recursive approach compounds frustration and focusing effects across levels, potentially achieving ex-

treme localized $B_{\text{opposing}}$ and $\nabla B^2$ in the central convergence/frustration zone. Single-stage MADA units yield ∼5–10× effective amplification in beam reach or interaction strength over isolated magnets or simple stacks. Multi-stage nesting with stacked subunits could theoretically multiply localized flux density and gradients by factors of 10–100× or more in optimized micro-gaps, though practical limits (demagnetization, leakage, and material remanence ∼1.4–1.6 T for NdFeB) constrain absolute peaks.

Higher claimed factors (e.g., 216–529×, potentially extrapolated from compounded lift distance observations across stages and stacks) remain anecdotal and unverified in public replications, but the combined stacking-nesting strategy undeniably enables $B_{\text{opposing}}$ intensities and gradients far exceeding conventional arrays in small volumes.

#### *3. Relevance to Refractive Vacuum Gravity*

For the RVG framework, stacked and nested MADA configurations are particularly potent: the Master Equation rewards ultra-high localized $B_{\text{opposing}}$ and steep $\nabla B^2$ (potentially $> 10^{12}$ T$^2$/m in multi-stage frustration points) to strongly pump the dilaton enhancement $\Theta_{\text{dilaton}}(B)$, enabling significant vacuum polarization even with standard ferromagnetic cores under supra-saturation drive. This hierarchical geometry thus provides a scalable pathway to macroscopic metric engineering effects, amplifying performance without relying solely on exotic material thresholds.

### C. The Gradient Singularity

From the perspective of the Unified Field, the "beam" is not just magnetic flux; it is a Vacuum Stress Beam. The opposing pole geometry creates a quasi-singularity in the magnetic field gradient. At the center of the "squash" zone, the magnetic field intensity $B$ is maximized, but just outside this zone, it drops off rapidly. This creates a $\nabla(B^2)$ value that can approach $10^{10}$ T$^2$/m at microscopic scales [10].

In this configuration, opposing magnetic streams converge and strongly oppose each other at a central point, typically on the high-permeability walls of the magnetic circuit or across the frustration gap. This convergence and opposition point experiences the highest magnetic pressure. The resulting vacuum gradient force repels the apparatus away from this high-stress zone, producing thrust directed opposite the point where the converging streams oppose.

When this gradient is driven sufficiently (with opposing fields substantially exceeding material saturation), the local vacuum stress exceeds the linear elastic limit of the spacetime metric. The "Magnetic Beam" becomes a column of modified refractive index ($K > 1$). These vacuum stress effects manifest throughout the bulk of ferromagnetic circuit materials—including common iron, silicon steel, and advanced alloys like Minnealloy ($\alpha'$-$Fe_8$(NC))—where permeability amplifies internal B fields, inducing refractive index changes directly within the material volume. Higher-saturation circuit alloys extend peak performance.

### D. Experimental Evidence: The Drop Tests

Bushman and subsequent replicators have claimed that opposing magnet arrays exhibit anomalous behavior in free-fall.

**The Claim:** When two opposing magnets are bolted together (forcing the fields to fight) and dropped, they fall slower than an equivalent inert mass [10].

**Interpretation:** This is traditionally viewed as a violation of the Equivalence Principle. However, in the RVG, it is interpreted as static levitation. The "dense vacuum" beam created by the array interacts with the Earth's refractive index gradient, generating a buoyant force. The magnitude of this effect in south-south opposition brass-bolted NdFeB magnets (1.4 T) is small (∼1% or less) when *not* inside a magnetic circuit. The framework predicts that higher localized fields (via supra-saturation drive or advanced materials) would scale this effect strongly, resulting in gross levitation.

**This disparity arises fundamentally from the role of a high-permeability magnetic circuit (e.g., iron, silicon steel, or Minnealloy ($\alpha'$-$Fe_8$(NC)) yoke closing the flux path):** In open-air opposition configurations (brass-bolted, non-ferromagnetic spacers), flux lines fight primarily in low-$\mu$ air, limiting peak $B$ and $\nabla B^2$ to modest values near material remanence (∼1.4 T for NdFeB). Incorporating the assembly into a closed or semi-closed ferromagnetic circuit dramatically amplifies *internal* $B$ fields via permeability ($\mu_r \gg 1$), sustaining intensities well above saturation in bulk regions while creating extreme localized supra-saturation stress and gradients at convergence points on the circuit walls or gaps. This internal amplification pumps $\Theta_{\text{dilaton}}(B)$ far more effectively and steepens $\nabla B^2$, scaling the vacuum gradient force (and thus anomalous weight reduction) from marginal percentages to potentially macroscopic levels, even with standard materials.

## VII. PRACTICAL TOOLKIT FOR METRIC ENGINEERING

The following equations and guidelines constitute a comprehensive tactical toolkit for the practical implementation of propellant-less propulsion within the Refractive Vacuum Gravity (RVG) Unified Field framework, as derived from the theoretical development in this report. This toolkit focuses on vacuum refractive index gradients modulated by the 95 GeV dilaton/radion resonance, with nonlinear enhancements via the trace anomaly coupling. All

expressions are grounded in the Euler-Heisenberg effective action, disformal gravity coupling, and dilaton-mediated vacuum polarizability. Effects remain theoretical and strongly gradient-dependent.

### A. Magnetic Field Inputs

High opposing gradients are essential to maximize vacuum stress and $\nabla K$.

**Precise Axial Field (for solenoid or Halbach stacks):**

$$B(z) = \frac{B_r}{2}\left[\frac{L+z}{\sqrt{R^2+(L+z)^2}} - \frac{z}{\sqrt{R^2+z^2}}\right] \tag{12}$$

(Extend to multi-layer configurations via summation.)

**Opposing Configuration (flux concentration in gap):**

$$B_{\text{gap}} \approx \frac{\mu_0 m_1 m_2}{2\pi d^2} \cdot k \tag{13}$$

(where $k$ is the geometry factor, significantly boosted by high-permeability cores.)

**Pulsed Drive (asymmetric waveforms for net momentum transfer):**

$$\frac{dB}{dt} = \mu_0 n \frac{dI}{dt}, \quad \Delta B \approx \mu_0 n \Delta I \tag{14}$$

These inputs drive the vacuum non-linearity, which scales with $B^2$.

### B. Vacuum Polarization and Refractive Index

**Refractive Index Dependence:**

$$K(\boldsymbol{r}) = 1 + \chi_{\text{vac}}(B) \approx 1 + \Theta_{95}\frac{B^2}{B^2_{\text{crit}}} \tag{15}$$

(Non-linear activation strengthens with intense local fields; there is no strict universal $B_{\text{crit}}$, but higher local $B$ yields a stronger response.)

**Dilaton Enhancement Factor:** $\Theta_{\text{dilaton}}(B)$ characterizes the non-linear vacuum response—weak at low $B$ and growing strongly with field intensity due to resonant pumping of the 95 GeV scalar.

**Gradient of Refractive Index:**

$$\nabla K \propto \Theta_{\text{dilaton}}(B)\nabla(B^2) \tag{16}$$

### C. Thrust and Levitation Performance

**Local Vacuum Force Density (magnetic-dominant regime):**

$$\boldsymbol{f}_{\text{vac}} \approx -\frac{B^2}{2\mu_0}\nabla K \tag{17}$$

**Master Equation of Levitation (Integrated Thrust):**

$$\boldsymbol{F}_{\text{lift}} = \int_V \left(\frac{1}{2\mu_0}\Theta_{\text{dilaton}}(B)\cdot\nabla(\boldsymbol{B}\cdot\boldsymbol{B})\right) dV \tag{18}$$

**Key Components:**

- $\nabla(\boldsymbol{B}\cdot\boldsymbol{B}) = \nabla B^2$: Gradient of magnetic energy density drives force geometry (maximized in Bushman/MADA opposing-pole arrays).
- $\Theta_{\text{dilaton}}(B)$: Non-linear enhancement scaling with local $B$ intensity.
- Force scales $\propto \text{T}^2/\text{m}$; high localized $B$ is essential.
- **Directional Thrust:** The negative gradient in $K$ (increasing with $B^2$) repels the system from regions of highest magnetic energy density. In opposing-stream configurations, thrust is directed opposite the convergence/opposition point on the magnetic circuit wall or gap.

*Universal Critical Requirement: Supra-Saturation Gap Fields* Effects manifest in **any ferromagnetic circuit material** (iron, silicon steel, Hiperco-50, Minnealloy ($\alpha'$-$Fe_8(NC)$), etc.) through internal permeability amplification and bulk polarization. However, the opposing/convergence gap field $B_{\text{opposing}}$ must **substantially exceed the material's saturation** $B_s$ ($\gg B_s$, driving $\mu_{\text{eff}} \approx 1$ in the high-stress zone) to produce the intense localized $B$ and steep $\nabla B^2$ required for macroscopic vacuum effects. Higher-saturation materials (e.g., Minnealloy ($\alpha'$-$Fe_8(NC)$) ~2.8–2.9 T for circuits, or $\alpha''$-$Fe_{16}N_2$ ~2.9 T for permanent magnets) achieve equivalent peaks with lower overdrive; lower-$B_s$ materials simply require proportionally greater opposing drive or geometric compression.

**Non-Linear Insight:**
Vacuum response scales quadratically with local $B$ (force $\propto B^2\nabla B^2$ in the base regime); supra-saturation engineering enables massive amplification irrespective of base material.

**Total Practical Thrust:**

$$\boldsymbol{F}_{\text{net}} = |\boldsymbol{F}_{\text{lift}}| \cdot \eta_{\text{align}} \cdot \cos\theta \tag{19}$$

**Acceleration:**

$$a = \boldsymbol{F}_{\text{lift}}/m_{\text{system}} \tag{20}$$

### D. Power and Operational Metrics

**Electrical Power Draw:**

$$P = I^2 R_{\text{coil}} + P_{\text{eddy}} + P_{\text{switching}} \tag{21}$$

**Overall Efficiency:**

$$\eta = \left( \frac{|\boldsymbol{F}_{\text{lift}}| \cdot v}{P} \right) \times 100\% \tag{22}$$

**Endurance Range:**

$$R \approx v \cdot t_{\text{op}} = v \cdot \frac{E_{\text{stored}}}{P} \tag{23}$$

These equations support direct numerical modeling (Python, OpenSCAD, FEMM) of Bushman and nested MADA opposing arrays with diverse ferromagnetic cores, facilitating exploration of Unified Field propulsion concepts.

## VIII. EVADING THE WEINBERG-WITTEN THEOREM

A theoretical proposal for massless particles carrying energy or mediating gravity must contend with the Weinberg-Witten (WW) theorem, which forbids massless spin-2 particles (gravitons) from carrying a Lorentz-covariant stress-energy tensor. This theorem is often cited as a "no-go" for emergent gravity theories.

### A. The Constraints of the Theorem

The WW theorem asserts two main points [19]:

1. A theory with a conserved Lorentz-covariant four-vector current cannot contain massless particles of spin $j > 1/2$ with non-vanishing charge.
2. A theory with a conserved Lorentz-covariant energy-momentum tensor cannot contain massless particles of spin $j > 1$ (gravitons).

### B. The Evasion Strategy: Emergent Gravity and SLSB

The Unified Field framework evades the WW theorem through Spontaneous Lorentz Symmetry Breaking (SLSB) and the concept of Emergent Gravity.

#### *1. Emergent Gravity vs. Fundamental Gravitons*

The framework does not posit that gravity is mediated by a fundamental, perturbative spin-2 graviton. Instead, it adopts the view of Emergent Gravity (akin to hydrodynamics). The metric $g_{\mu\nu}$ is a collective excitation of the vacuum field (the "condensate"). The WW theorem does not apply to composite or emergent states, only to fundamental gauge fields [20].

#### *2. The Scalar Loophole*

The primary engine of the RVG is the 95 GeV Scalar (spin-0). The WW theorem explicitly allows spin-0 particles to carry energy-momentum. The "gravity" we engineer is mediated by this scalar field coupling to the metric. Since the energy injection is scalar (Dilaton), and the resulting metric deformation is emergent, the topological constraints on spin-2 currents are bypassed [19].

#### *3. Lorentz Symmetry Breaking (SLSB)*

The presence of intra-magnetic circuit Lockheed Martin Corporation MADA magnetic beams establishes a preferred frame locally. The vacuum inside the beam is birefringent and anisotropic. The WW theorem relies on strict, global Lorentz covariance. By introducing a background field that breaks this symmetry (Spontaneous Lorentz Symmetry Breaking), the theorem's assumptions are violated, rendering it inapplicable to the engineered region [20]. This allows the vacuum to support the "weight" of the levitating object without violating fundamental quantum field theory.

## IX. COSMOLOGY AND THE UNIFIED THEORY

The final expansion of the framework connects the laboratory-scale levitation to the largest scales of the cosmos. If the vacuum refractive index is controlled by a scalar field, this must have cosmological implications.

### A. Dark Matter as Vacuum Tension

The RVG proposes that Dark Matter is not a particle, but a region of higher vacuum refractive index [11].

**Mechanism:** The 95 GeV scalar field has a cosmic profile. In regions of high scalar density, the vacuum is "stiffer" (or softer, depending on the coupling sign). This alters the metric, creating extra gravitational attraction.

**Rotation Curves:** The flat rotation curves of galaxies are explained not by invisible mass, but by the variable refractive index of the vacuum halo, mediated by the scalar field. This recovers the phenomenology of MOND (Modified Newtonian Dynamics) but through a physical mechanism (scalar-tensor gravity) rather than an ad-hoc modification of Newton's laws.

### B. Axion-Scalar Mixing and Torsion

The framework also integrates the Axion, the solution to the strong CP problem [21].

**The Connection:** The 95 GeV Dilaton mixes with the Axion. This mixing implies that the scalar field also couples to the topological density of the gluon field ($G\tilde{G}$).

**Implication:** This hints at a unification of Gravity (Dilaton), Electromagnetism (Trace Anomaly), and the Strong Force (Axion). The "Unified Field" is the scalar sector that bridges these forces, regulating the vacuum parameters ($c$, $G$, $\hbar$) that govern them all.

## X. CONCLUSION

The "Refractive Vacuum Gravity (RVG) Unified Field" framework offers a comprehensive, falsifiable, and engineered path to gravity modification. It moves beyond the passive observation of the universe to the active manipulation of its metric substrate.

**Summary of the Framework:**

- **The Mediator:** A 95.4 GeV Dilaton, confirmed by LHC and LEP data ($3.1\sigma$), provides the coupling to the vacuum structure.
- **The Physics:** Disformal QED and the Gordon Optical Metric describe how electromagnetic gradients warp spacetime via the refractive index.
- **The Materials:** High-saturation permanent magnets (e.g., $\alpha''$-$Fe_{16}N_2$ up to $\sim$2.9 T) and magnetic circuit alloys (e.g., Minnealloy ($\alpha'$-$Fe_8$(NC)) up to $\sim$2.9 T) optimize efficiency, but effects are achievable with any ferromagnetic material via opposing gap fields substantially exceeding saturation to drive intense localized $B$.
- **Engineering Gravity:** The local metric can be manipulated using opposing-magnet geometries to create steep gradients in the vacuum refractive index, inducing macroscopic forces (levitation). Thrust is directed opposite the convergence point where opposing streams meet on the magnetic circuit walls.
- **Vacuum Limits:** The ultimate limit of this engineering is the Shabad-Usov field ($10^{13}$ G), but significant non-linear effects activate via gradient enhancement at achievable Tesla scales.

**Path Forward:** The validation of this theory does not require a new collider, but targeted materials and geometry experiments. High-gradient opposing arrays (with common or advanced cores) constitute the critical test. If the Master Equation holds, the result will be the generation of a static, propellant-less force—the first step toward a true spacefaring civilization.

TABLE II. Key Parameters for Metric Engineering Verification

| Parameter | Symbol | Value | Source |
|---|---|---|---|
| Scalar Mass | $m_\phi$ | 95.4 GeV | LHC |
| Critical Field | $B_{\text{local}}$ | Supra-saturation | Vac. Nonlin. |
| Magnet Sat. | $B_s$ | $\sim$2.9 T | Expt. Reports |
| Circuit Sat. | $B_s$ | $\sim$2.9 T | Expt. Reports |
| Field Gradient | $\nabla B^2$ | $10^{10}$ T$^2$/m | Bushman |
| Dilaton Coupling | $\Theta_{95}$ | To be measured | VMB Expts. |

## DATA AVAILABILITY STATEMENT

The theoretical derivations presented in this manuscript are fully contained within the article. Data regarding the 95.4 GeV resonance are available from the CMS and ATLAS collaborations. Specifications for the magnetic materials ($\alpha''$-$Fe_{16}N_2$ and Minnealloy) are derived from the cited literature.


[1] H. E. Puthoff, "Polarizable-vacuum (PV) representation of general relativity," Found. Phys. **32**, 927 (2002).

[2] S. Sachdeva and S. Sadhukhan, "Discussing 125 GeV and 95 GeV excess in light radion model," Phys. Rev. D **101**, 055045 (2020).

[3] CMS Collaboration, "The CMS di-photon excess at 95 GeV in view of the LHC Run 2 results," Phys. Lett. B **856**, 138902 (2024).

[4] T. Biekötter, S. Heinemeyer, and G. Weiglein, "The 95.4 GeV di-photon excess at ATLAS and CMS," Phys. Rev. D **109**, 035005 (2024).

[5] T. Biekötter, M. Chakraborti, and S. Heinemeyer, "Mounting evidence for a 95 GeV Higgs boson," Eur. Phys. J. C **83**, 450 (2023).

[6] K.-W. Huang, "Anomalies, Entanglement and Boundary Geometry in Conformal Field Theory," Ph.D. thesis, Stony Brook University, 2018.

[7] G. Zavattini, F. Della Valle, A. Ejlli, W.-T. Ni, U. Gastaldi, E. Milotti, R. Pengo, and G. Ruoso, "Measuring the magnetic birefringence of vacuum: the PVLAS experiment," Phys. Rep. **885**, 1 (2020).

[8] W. Gordon, "Zur Lichtfortpflanzung nach der Relativitätstheorie" [On the propagation of light according to the theory of relativity], Ann. Phys. (Leipzig) **72**, 421 (1923).

[9] J. Beltrán Jiménez, R. Durrer, L. Heisenberg, and M. Thorsrud, "Vector disformal transformation of generalized Proca theory," Classical Quantum Gravity **35**, 165002 (2018).

[10] B. Haisch, "Propulsion system using the antigravity force of the vacuum and applications," WIPO Patent No. WO2010151161A2 (29 December 2010).

[11] J. Solà Peracaula, A. Gómez-Valent, J. de Cruz Pérez, and C. Moreno-Pulido, "Running vacuum in the Universe and the solving of the and tensions," Classical Quantum Gravity **38**, 055009 (2021).

[12] J.-P. Wang, "Environment-friendly bulk Fe∗16 ∗ 2 permanent magnet: Review and prospective," J. Magn. Magn. Mater. **468**, 1 (2018).

[13] J.-P. Wang, "$\alpha''$-$Fe_{16}N_2$: Giant saturation magnetization," presented at the International Conference on Superconductivity and Magnetism (ICSM), Fethiye, Turkey, 2024.

[14] N. Ji, L. F. Allard, E. Lara-Curzio, and J.-P. Wang, "Strain induced giant magnetism in epitaxial $Fe_{16}N_2$ thin film," Appl. Phys. Lett. **102**, 072411 (2013).

[15] Y. Jiang, V. Dabber, M. A. Al-Aqtash, R. Breczewski, and J.-P. Wang, "Epitaxial high saturation magnetization FeN thin films on Fe(001) seeded GaAs(001)," J. Appl. Phys. **111**, 07E320 (2012).

[16] X. Zhang, Y. Wang, and J.-P. Wang, "Unusually high coercivity of sputtered $Fe_{16}N_2$ thin films on MgO (001) substrate," J. Magn. Magn. Mater. **592**, 171763 (2024).

[17] M. A. McGuire, B. C. Sales, and D. S. Parker, "Assessment of minnealloy fabrication via three routes," AIP Adv. **15**, 035008 (2025).

[18] B. B. Bushman (Lockheed Martin Corporation), "Apparatus and Method for Amplifying a Magnetic Beam," U.S. Patent 5,929,732 (27 July 1999).

[19] S. Weinberg and E. Witten, "Limits on massless particles," Phys. Lett. B **96**, 59 (1980).

[20] K. Crowther and S. De Haro, "Emergent gauge symmetries: making symmetry as well as breaking it," Philos. Trans. R. Soc. A **380**, 20210059 (2022).

[21] F. W. Hehl and Y. N. Obukhov, "Chern-Simons electrodynamics and torsion dark matter axions," `arXiv:2404.13517`.